

## $^{51}\text{V}$ NMR Studies of Crystalline Divalent Metal Vanadates and Divanadates

Satoshi HAYAKAWA, Toshinobu YOKO,\* and Sumio SAKKA  
Institute for Chemical Research, Kyoto University, Uji, Kyoto 611

(Received June 2, 1993)

$^{51}\text{V}$  static and magic-angle spinning (MAS) NMR spectra of crystalline divalent metal vanadates,  $\text{M}_3(\text{VO}_4)_2$  ( $\text{M}=\text{Mg}, \text{Sr}, \text{Ba}, \text{Zn}, \text{Pb}$ ) and  $\text{Mg}_2\text{M}'(\text{VO}_4)_2$  ( $\text{M}'=\text{Sr}, \text{Ba}, \text{Pb}$ ) and divanadates,  $\text{M}_2\text{V}_2\text{O}_7$  ( $\text{M}=\text{Mg}, \text{Ca}, \text{Sr}, \text{Ba}, \text{Zn}, \text{Pb}$ ) have been measured. In vanadates and dichromate-type divanadates, the  $^{51}\text{V}$  isotropic chemical shifts decrease linearly with decreasing electronegativity of divalent metal atom adjacent to the  $\text{VO}_4$ -tetrahedron. This was interpreted by considering that the electron density and the symmetry of  $\text{VO}_4$ -tetrahedron increases with decreasing electronegativity of divalent metal atom. This effect was more significant in vanadates than in divanadates. In divanadates the isotropic chemical shifts of the thortveitite-type configuration appeared at lower frequencies than that of the dichromate-type configuration. This was explained by assuming that the degree of s-hybridization of the oxygen orbitals in the V–O–V bonds is higher in the thortveitite-type than in the dichromate-type.

Crystalline and amorphous vanadates have been studied extensively due to possible applications as catalysts for oxidation of hydrocarbons and alcohols, switching elements,<sup>1)</sup> solid electrolytes in the lithium secondary batteries, counterelectrodes in electrochromic devices<sup>2,3)</sup> and non-linear optical elements.<sup>4,5)</sup> In order to understand the chemical and physical properties of vanadium compounds involved in those applications, it is of substantial importance to elucidate the local environment of a vanadium atom in vanadates.

It is well recognized that a multinuclear NMR is a powerful tool to reveal the detailed local structure of a given nucleus of interest.  $^{51}\text{V}$  has a nuclear quadrupole moment (eQ) which interacts with the electric field gradients caused by an asymmetric electric field around the nucleus because  $I=7/2$ . Such a quadrupole interaction causes the broadening of the observed NMR peak and the low-frequency shifts of the peak position compared to the isotropic chemical shift. However, the use of the high magnetic field and magic-angle spinning (MAS) can decrease the quadrupole interaction to a negligible order of magnitude.<sup>6)</sup> Accordingly, the  $^{51}\text{V}$  NMR technique using high magnetic fields has been applied to the structural studies on alkali and alkaline earth vanadates,<sup>7–9)</sup> so far.

There have been few comprehensive studies, however, which aim at establishing the relationships between crystallographic parameters and  $^{51}\text{V}$  NMR spectral parameters, such as isotropic chemical shift, chemical shift anisotropy, and asymmetry parameter in crystalline vanadates. In the present work, systematic measurements have been made on the  $^{51}\text{V}$  static and MAS NMR spectra of crystalline divalent metal vanadates with a known crystal structure and the isotropic chemical shift, the chemical shift anisotropy, and the asymmetry parameter have been determined. Based on the relationships between crystallographic parameters of the vanadates and  $^{51}\text{V}$  NMR parameters, the effects of divalent metals (Mg, Ca, Sr, Ba, Zn, and Pb) on the local environment of a vanadium atom are discussed.

## Experimental

**Sample Preparation.** Crystalline vanadates studied were divalent metal vanadates,  $\text{M}_3(\text{VO}_4)_2$  ( $\text{M}=\text{Mg}, \text{Sr}, \text{Ba}, \text{Zn}, \text{Pb}$ ) and  $\text{Mg}_2\text{M}'(\text{VO}_4)_2$  ( $\text{M}'=\text{Sr}, \text{Ba}, \text{Pb}$ ) and divanadates,  $\text{M}_2\text{V}_2\text{O}_7$  ( $\text{M}=\text{Mg}, \text{Ca}, \text{Sr}, \text{Ba}, \text{Zn}, \text{Pb}$ ). In this paper,  $\text{M}_3(\text{VO}_4)_2$  stands for vanadates and  $\text{Mg}_2\text{M}(\text{VO}_4)_2$  for vanadates in which two of divalent metal atoms are Mg and the rest is another divalent metal atom such as Sr, Ba or Pb.  $\text{M}_2\text{V}_2\text{O}_7$  stands for divanadates. All the crystalline vanadates were prepared from the reagent grade chemicals,  $\text{V}_2\text{O}_5$ , MgO,  $\text{SrCO}_3$ ,  $\text{BaCO}_3$ ,  $\text{CaCO}_3$ , ZnO, and PbO, supplied by Nacalai Tesque and Wako Chemicals. Crystalline  $\text{Sr}_3(\text{VO}_4)_2$ ,  $\text{Pb}_3(\text{VO}_4)_2$ ,  $\text{Mg}_2\text{Sr}(\text{VO}_4)_2$ , and  $\text{Mg}_2\text{Pb}(\text{VO}_4)_2$  were synthesized by crystallization from the melts. Other crystals were synthesized by solid-state reaction of the starting powder mixture. The crystalline phases of all the samples were identified by comparing their powder X-ray diffraction patterns with the data of JCPDS-FILE.

**NMR Measurements.**  $^{51}\text{V}$  static and MAS NMR spectra of powdered crystalline vanadates were recorded at 105 MHz (9.4 Tesla) on a JEOL JNM-GSX400MAS FT-NMR spectrometer. A single pulse sequence was used; the pulse length of 0.5–2.0  $\mu\text{s}$  corresponding to a flip angle of ca.  $22.5^\circ$ , the pulse delay of 1 s and the accumulation of 400–1000 scans. A cylindrical zirconia rotor was rotated at a speed of about 6 kHz in the  $^{51}\text{V}$  MAS NMR measurements. The  $^{51}\text{V}$  MAS NMR spectra were obtained at two rotation rates in the range 4–6 Hz to discriminate between the main peak and spinning side bands. The peak whose position does not change with the rotation rate can be taken as a main peak which gives an isotropic chemical shift. The  $^{51}\text{V}$  NMR chemical shift expressed in terms of the  $\delta$  scale with respect to  $\text{Zn}_3(\text{VO}_4)_2$  used as the second external reference which is assumed to have  $\delta=-522$  ppm.<sup>8)</sup> Accordingly, the  $^{51}\text{V}$  NMR chemical shifts are presented with reference to  $\text{VOCl}_3$  neat liquid which is assumed to have  $\delta=0$  ppm. The right-hand side of the horizontal axis corresponds to the lower resonance frequency.

Generally a line broadening in the static NMR spectra is caused by chemical shift anisotropy, dipole–dipole interaction and quadrupolar interaction. The use of higher magnetic field increases the chemical shift anisotropy while it

decreases the quadrupolar interaction.<sup>7)</sup> The line broadening due to chemical shift anisotropy gives a typical powder pattern arising from an isotropic distribution of the direction of principal axes of the chemical shift tensor with respect to the external magnetic field.<sup>20)</sup> The theoretical spectrum can be calculated from the following equations given by Bloembergen et al.<sup>21)</sup> under the condition that the principal components of the chemical shift tensors  $\sigma_1$ ,  $\sigma_2$ , and  $\sigma_3$  are in the order,  $\sigma_3 > \sigma_2 > \sigma_1$ , for  $\sigma_3 > \sigma > \sigma_2$

$$I(\sigma) = \frac{1}{\pi} \{(\sigma - \sigma_1)(\sigma_3 - \sigma_2)\}^{-1/2} K(m) \quad (1)$$

$$m = \frac{(\sigma_2 - \sigma_1)(\sigma_3 - \sigma)}{(\sigma_3 - \sigma_2)(\sigma - \sigma_1)} \quad (2)$$

for  $\sigma_2 > \sigma > \sigma_1$

$$I(\sigma) = \frac{1}{\pi} \{(\sigma_3 - \sigma)(\sigma_2 - \sigma_1)\}^{-1/2} K(m) \quad (3)$$

$$m = \frac{(\sigma - \sigma_1)(\sigma_3 - \sigma_2)}{(\sigma_3 - \sigma)(\sigma_2 - \sigma_1)} \quad (4)$$

for  $\sigma > \sigma_3, \sigma > \sigma_1$

$$I(\sigma) = 0 \quad (5)$$

and

$$K(m) = \int_0^{\frac{\pi}{2}} \frac{d\theta}{\sqrt{1 - m^2 \sin^2 \theta}} \quad (6)$$

The values  $\sigma_1$ ,  $\sigma_2$ , and  $\sigma_3$  are estimated by fitting the theoretical spectra to the static spectra. The simulated spectra are obtained by convoluting a broadening function (Lorentz function) into the theoretical spectra as follows;

$$I(\sigma') = \frac{1}{N} \int_{-\infty}^{+\infty} \frac{I(\sigma)}{H_w^2 + (\sigma' - \sigma)^2} d\sigma \quad (7)$$

where  $I(\sigma')$  is the broadened powder pattern giving the simulated spectrum,  $N$  the normalization factor and  $H_w$  the line width.

The chemical shift anisotropy,  $\Delta\delta$ , and the asymmetry parameter,  $\eta$ , can be determined by using the following definitions,<sup>9,19)</sup>

$$\Delta\delta = \delta_3 - \frac{\delta_1 + \delta_2}{2} \quad (8)$$

$$\eta = \frac{\delta_2 - \delta_1}{\delta_3 - \delta_{\text{iso(static)}}} \quad (9)$$

$$\delta_{\text{iso(static)}} = \frac{\delta_1 + \delta_2 + \delta_3}{3} \quad (10)$$

where  $\delta_{\text{iso(static)}}$  is the isotropic chemical shift determined from  $^{51}\text{V}$  static NMR and  $\delta_1$ ,  $\delta_2$ ,  $\delta_3$  are the principal components of chemical shift tensors. The principal components of the chemical shift tensors can be determined based on Eq. 11.

$$|\delta_3 - \delta_{\text{iso(static)}}| \geq |\delta_1 - \delta_{\text{iso(static)}}| \geq |\delta_2 - \delta_{\text{iso(static)}}| \quad (11)$$

The asymmetry parameter,  $\eta$ , is a measure of the deviation of chemical shift tensors from the axial symmetry;  $\eta=0$  for axially symmetric electronic distribution around a vanadium atom and  $\eta=1$  for axially asymmetric distribution.

## Results

All the crystalline vanadates prepared in the present study had the identical X-ray powder diffraction patterns to those in the JCPDS-FILE. All the samples had no extra diffraction peaks, showing that they consist of a single phase.

Table 1 gives the crystallographic parameters of the crystalline vanadates; the point symmetry of  $\text{VO}_4$ -tetrahedron expressed by Schoenflies symbol and the V-O-V angle, the average V-O bond length ( $<2.2 \text{ \AA}$ ) and the average angle of twist relative to the V-V axis in  $\text{V}_2\text{O}_7^{4-}$  anion.<sup>10-18)</sup> The degree of the structural distortion of  $\text{VO}_4$ -tetrahedron in the first coordination sphere of a vanadium atom is expressed by the following two crystallographic parameters;

$$\Delta d_n = \sum |(V-O)_d - \overline{(V-O)}_d| / 4 \quad (12)$$

$$\Delta a_n = \sum |(O-V-O)_a - \overline{(O-V-O)}_a| / 6 \quad (13)$$

where  $(V-O)_d$  is the V-O bond length,  $\overline{(V-O)}_d$  the average V-O bond length,  $(O-V-O)_a$  the O-V-O bond angle and  $\overline{(O-V-O)}_a$  the average O-V-O bond angle. In Fig. 1 the  $\Delta a_n$  is plotted against the  $\Delta d_n$ . This shows that the  $\Delta a_n$  increases with increasing  $\Delta d_n$  except for  $\text{Mg(2)}$ . Since the vanadium site indicated by  $\text{Mg(2)}$  is regarded as an intermediate between  $\text{VO}_4$ -tetrahedron and  $\text{VO}_5$ -trigonal bipyramid as will be stated in the fol-

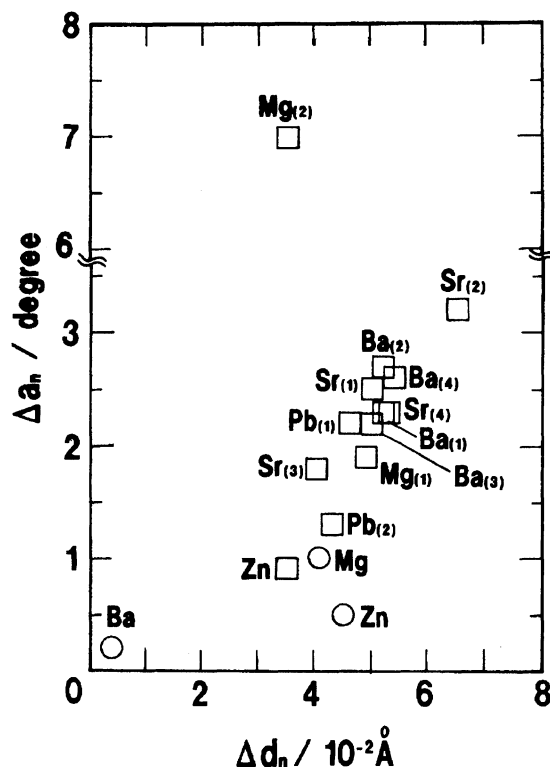


Fig. 1. Plots of the  $\Delta d_n$  vs. the  $\Delta a_n$  for vanadates (○) and divanadates (□). The numerals in the parentheses denote the vanadium site number of the unit cell.

Table 1. Local Symmetry of VO<sub>4</sub>-Tetrahedron, Average V–O Bond Length, V–O–V Angle, Average Angle of Twist in Alkaline Earth and Other Divalent Metal Vanadates and Divanadates Calculated from Reference Data<sup>10–18)</sup>

Compound	Local point symmetry	Site No.	Average V–O bond length/Å	$\Delta d_n$ 10 <sup>–2</sup> Å	$\Delta a_n$ degree	V–O–V angle degree	Average angle of twist/degree
<b>Vanadate</b>							
Mg <sub>3</sub> (VO <sub>4</sub> ) <sub>2</sub>	<i>C<sub>s</sub></i>	—	1.73	4.0	1.0	—	—
Sr <sub>3</sub> (VO <sub>4</sub> ) <sub>2</sub>	—	—	1.706	0.4	0.2	—	—
Zn <sub>3</sub> (VO <sub>4</sub> ) <sub>2</sub>	<i>C<sub>s</sub></i>	—	1.72	4.5	0.5	—	—
Pb <sub>3</sub> (VO <sub>4</sub> ) <sub>2</sub>	—	—	—	—	—	—	—
Mg <sub>2</sub> Sr(VO <sub>4</sub> ) <sub>2</sub>	—	—	—	—	—	—	—
Mg <sub>2</sub> Ba(VO <sub>4</sub> ) <sub>2</sub>	—	—	—	—	—	—	—
Mg <sub>2</sub> Pb(VO <sub>4</sub> ) <sub>2</sub>	—	—	—	—	—	—	—
<b>Divanadate</b>							
Mg <sub>2</sub> V <sub>2</sub> O <sub>7</sub>	<i>E</i>	1	1.71	4.9	1.9	140.6	53(1) <sup>a)</sup>
	<i>E</i> (VO <sub>4</sub> )	2	1.73	3.5	7.0	—	—
	<i>E</i> (VO <sub>5</sub> ) <sup>b)</sup>	2	1.87	18.9	14.8	—	—
Ca <sub>2</sub> V <sub>2</sub> O <sub>7</sub>	—	—	—	—	—	—	—
Sr <sub>2</sub> V <sub>2</sub> O <sub>7</sub>	<i>E</i>	1	1.71	5.0	2.5	122	6(3) <sup>a)</sup>
	<i>E</i>	2	1.73	6.5	3.2	—	—
	<i>E</i>	3	1.73	4.0	1.8	124	—
	<i>E</i>	4	1.73	5.3	2.3	—	—
Ba <sub>2</sub> V <sub>2</sub> O <sub>7</sub>	<i>E</i>	1	1.715	5.2	2.3	125.6	9(7) <sup>a)</sup>
	<i>E</i>	2	1.721	5.2	2.7	—	—
	<i>E</i>	3	1.715	5.0	2.2	123.7	—
	<i>E</i>	4	1.724	5.4	2.6	—	—
Zn <sub>2</sub> V <sub>2</sub> O <sub>7</sub>	<i>E</i>	—	1.72	3.5	0.9	149.3	59(5) <sup>a)</sup>
Pb <sub>2</sub> V <sub>2</sub> O <sub>7</sub>	<i>E</i>	1	1.72	4.6	2.2	122	11(5) <sup>a)</sup>
	<i>E</i>	2	1.73	4.3	1.3	—	—

a) Estimated standard deviation. b) The 5th V–O bond is taken into consideration.

lowing discussion, such a difference in the coordination state is clearly reflected in the very large  $\Delta a_n$ . Therefore, it can be assumed that both the parameters exhibit the structural distortion of VO<sub>4</sub>-tetrahedron although for Mg(2) the situation is somewhat different.

Figure 2a shows the <sup>51</sup>V static NMR spectra of crystalline vanadates, M<sub>3</sub>(VO<sub>4</sub>)<sub>2</sub> (M=Mg, Sr, Ba, Zn, Pb). The figure shows that the <sup>51</sup>V static NMR spectrum of each crystalline vanadate consists of only one symmetrical peak. Figure 2b shows the <sup>51</sup>V MAS NMR spectra having a sharp peak for these crystalline vanadates. It is clearly seen that the peak position changes with the kind of divalent metal.

Figure 3 shows the <sup>51</sup>V static and MAS NMR spectra of crystalline vanadates, Mg<sub>2</sub>M'(VO<sub>4</sub>)<sub>2</sub> (M'=Sr, Ba, Pb) which contain two kinds of divalent metals. It is seen that the static NMR spectrum consists of a peak at lower frequencies and a shoulder at higher frequencies. On the other hand, each MAS NMR spectrum has only one main peak, of which the position shifts with the kind of substituted divalent metal. This indicates that these vanadates are single phase solid solutions and do not contain any other vanadates such as Sr<sub>3</sub>(VO<sub>4</sub>)<sub>2</sub>, Ba<sub>3</sub>(VO<sub>4</sub>)<sub>2</sub>, and Pb<sub>3</sub>(VO<sub>4</sub>)<sub>2</sub>.

Figure 4a shows the <sup>51</sup>V static NMR spectra of crystalline divanadates, M<sub>2</sub>V<sub>2</sub>O<sub>7</sub> (M=Mg, Ca, Sr, Ba, Zn, and Pb). The static NMR spectrum consists of a peak

at higher frequencies and a shoulder at lower frequencies except for Mg<sub>2</sub>V<sub>2</sub>O<sub>7</sub> and Zn<sub>2</sub>V<sub>2</sub>O<sub>7</sub>. The line width of the divanadates are much broader than those of the vanadates as in Fig. 2.

Figure 4b shows the <sup>51</sup>V MAS NMR spectra of these crystalline divanadates. The MAS NMR spectrum of Mg<sub>2</sub>V<sub>2</sub>O<sub>7</sub> consists of many sharp peaks. Two of them at  $\delta = -551$  and  $-647$  are found to be isotropic chemical shifts and others are spinning side bands (SSB). The MAS NMR spectra of Ca<sub>2</sub>V<sub>2</sub>O<sub>7</sub>, Zn<sub>2</sub>V<sub>2</sub>O<sub>7</sub>, and Pb<sub>2</sub>V<sub>2</sub>O<sub>7</sub> show only one isotropic chemical shift and several SSB's. On the other hand, there are four isotropic chemical shifts in Sr<sub>2</sub>V<sub>2</sub>O<sub>7</sub> ( $\delta = -561$ ,  $-581$ ,  $-584$ ,  $-593$ ) and three in Ba<sub>2</sub>V<sub>2</sub>O<sub>7</sub> ( $\delta = -579$ ,  $-589$ ,  $-599$ ).

Table 2 summarizes the chemical shift tensors,  $\delta_1$ ,  $\delta_2$ , and  $\delta_3$ , chemical shift anisotropy,  $\Delta\delta$ , and asymmetry parameter,  $\eta$ , of various crystalline vanadates and divanadates studied in the present paper. The difference in isotropic chemical shifts determined from MAS NMR spectra and static NMR spectra is less than 10 ppm, which is within the full width at half maximum of about 15 ppm obtained from the main peaks of MAS NMR spectra and within the experimental errors. For comparison, the isotropic chemical shifts of the vanadates (Mg<sub>3</sub>(VO<sub>4</sub>)<sub>2</sub>, Zn<sub>3</sub>(VO<sub>4</sub>)<sub>2</sub>) and divanadates (Zn<sub>2</sub>V<sub>2</sub>O<sub>7</sub>, Pb<sub>2</sub>V<sub>2</sub>O<sub>7</sub>) taken from Ref. 8 are also shown in Ta-

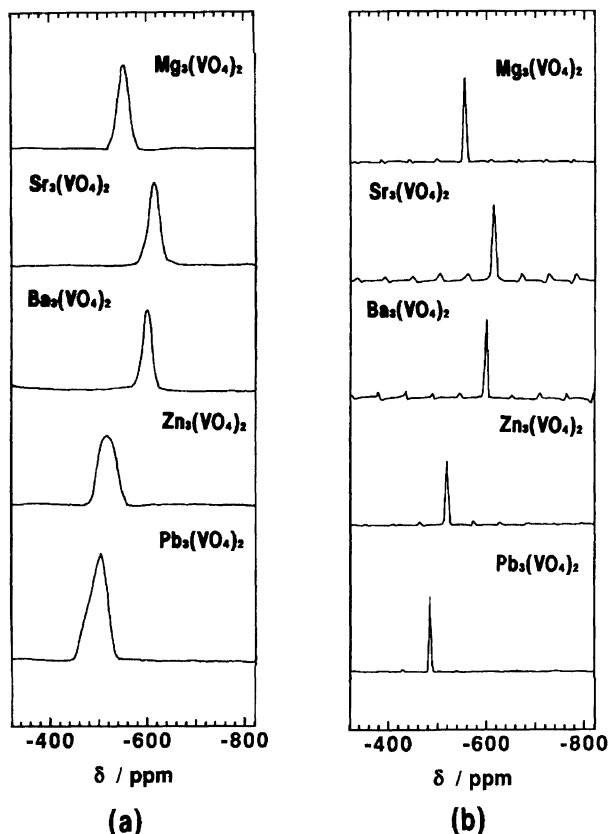


Fig. 2.  $^{51}\text{V}$  static (a) and MAS (b) NMR spectra of various crystalline vanadates.

ble 2, which were obtained from  $^{51}\text{V}$  MAS NMR experiments in a higher magnetic field, 11.7 Tesla. The difference in isotropic chemical shift between the present and reference data is less than 3 ppm. The agreement is excellent, indicating that in these crystalline vanadates the chemical shifts do not have any significant magnetic field dependence. In addition, the second quadrupolar shifts are estimated to be less than  $-7$  ppm,<sup>8)</sup> which is also within the experimental errors. Therefore, no correction for the second-order quadrupolar shifts was made in the present study. The asymmetry parameter,  $\eta$ , in the vanadates decreases in the order,  $\text{Mg}_3(\text{VO}_4)_2 > \text{Zn}_3(\text{VO}_4)_2 > \text{Ba}_3(\text{VO}_4)_2 > \text{Sr}_3(\text{VO}_4)_2 \gg \text{Pb}_3(\text{VO}_4)_2 > \text{Mg}_2\text{Sr}(\text{VO}_4)_2 \gg \text{Mg}_2\text{Pb}(\text{VO}_4)_2 > \text{Mg}_2\text{Ba}(\text{VO}_4)_2$ . In the divanadates the  $\eta$  decreases in the order;  $\text{Mg}_2\text{V}_2\text{O}_7$  (site 1)  $\approx$   $\text{Mg}_2\text{V}_2\text{O}_7$  (site 2)  $\approx$   $\text{Ca}_2\text{V}_2\text{O}_7 > \text{Zn}_2\text{V}_2\text{O}_7 \gg \text{Pb}_2\text{V}_2\text{O}_7 > \text{Sr}_2\text{V}_2\text{O}_7$  as shown in Table 2.

### Discussion

**Crystalline Vanadates.** It is well known that the isotropic chemical shift is very sensitive to the local environment of a nucleus including the nature of chemical bonds, the structural configuration around it and the degree of polymerization. In all vanadates and divanadates studied in the present paper, although a vanadium atom is tetrahedrally surrounded by four oxy-

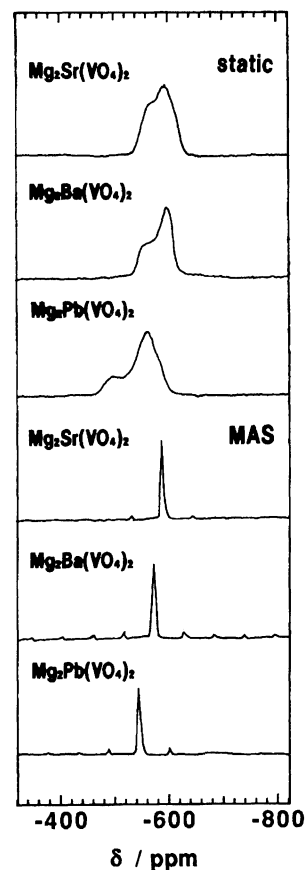


Fig. 3.  $^{51}\text{V}$  static and MAS NMR spectra of various crystalline vanadates.

gens, the V–O bond lengths and O–V–O bond angles are not the same. Since the charge on the vanadate group,  $\text{VO}_4^{3-}$ , and divanadate group,  $\text{V}_2\text{O}_7^{4-}$ , is compensated by the second neighboring cations, M, it is reasonable to assume that the  $^{51}\text{V}$  chemical shift is dependent on the nature of M, especially the electron-withdrawing power to oxygens, that is, the electronegativity of M. In Fig. 5 the  $^{51}\text{V}$  isotropic chemical shifts of vanadates determined by  $^{51}\text{V}$  MAS NMR are plotted against Pauling's electronegativity ( $EN$ ) of the divalent metal atom (M). A linear relationship is seen. The figure shows that the  $^{51}\text{V}$  isotropic chemical shift in vanadates decreases in the order  $\text{Pb}_3(\text{VO}_4)_2 > \text{Zn}_3(\text{VO}_4)_2 > \text{Mg}_3(\text{VO}_4)_2 > \text{Sr}_3(\text{VO}_4)_2 \approx \text{Ba}_3(\text{VO}_4)_2$ . The linear relationship between the isotropic chemical shift,  $\delta_{\text{iso}}$ , and the electronegativity,  $EN$ , is expressed by the following equation.

$$\delta_{\text{iso}} = 122 \times (EN - 5.88) \quad (14)$$

This indicates that the magnetic shielding of a vanadium atom is predominantly affected by the electron-withdrawing power of the second neighboring divalent metal atoms around the  $\text{VO}_4$ -tetrahedron and the electron density on the oxygen is larger in the order  $\text{Pb}_3(\text{VO}_4)_2 > \text{Zn}_3(\text{VO}_4)_2 > \text{Mg}_3(\text{VO}_4)_2 > \text{Ba}_3(\text{VO}_4)_2 >$

Table 2. Isotropic Chemical Shifts Determined by <sup>51</sup>V MAS NMR at 9.4 T and Shift Tensors,  $\delta_1$ ,  $\delta_2$ , and  $\delta_3$ , Chemical Shift Anisotropy;  $\Delta\delta$ , and Asymmetry Parameter;  $\eta$ , Determined by <sup>51</sup>V Static NMR

Compound	$\delta_{\text{iso(MAS)}}$	$\delta_{\text{iso(static)}}$	$\delta_1$	$\delta_2$	$\delta_3$	$\Delta\delta$	$\eta$
Vanadate							
Mg <sub>3</sub> (VO <sub>4</sub> ) <sub>2</sub>	-557 -554 <sup>a)</sup>	-557	-542	-557	-572	-23	1
Sr <sub>3</sub> (VO <sub>4</sub> ) <sub>2</sub>	-608	-617	-631	-619	-604	21	0.86
Ba <sub>3</sub> (VO <sub>4</sub> ) <sub>2</sub>	-603	-604	-593	-604	-616	-17	0.92
Zn <sub>3</sub> (VO <sub>4</sub> ) <sub>2</sub>	-522 -522 <sup>a)</sup>	-520	-493	-519	-548	-42	0.93
Pb <sub>3</sub> (VO <sub>4</sub> ) <sub>2</sub>	-486	-499	-521	-508	-467	48	0.41
Mg <sub>2</sub> Sr(VO <sub>4</sub> ) <sub>2</sub>	-581	-586	-617	-592	-548	57	0.66
Mg <sub>2</sub> Ba(VO <sub>4</sub> ) <sub>2</sub>	-575	-585	-606	-600	-547	56	0.16
Mg <sub>2</sub> Pb(VO <sub>4</sub> ) <sub>2</sub>	-549	-544	-574	-565	-493	77	0.18
Divanadate							
Mg <sub>2</sub> V <sub>2</sub> O <sub>7</sub>	-551 -647	-561 -655	-611 -717	-571 -667	542 -582	89 110	0.68 0.68
Ca <sub>2</sub> V <sub>2</sub> O <sub>7</sub>	-575	-575	-523	-565	-637	-93	0.68
Sr <sub>2</sub> V <sub>2</sub> O <sub>7</sub>	-561, -581, -584, -593	-589	-542	-552	-672	-125	0.12
Ba <sub>2</sub> V <sub>2</sub> O <sub>7</sub>	-579, -589, -599	—	—	—	—	—	—
Zn <sub>2</sub> V <sub>2</sub> O <sub>7</sub>	-620 -619 <sup>a)</sup>	-612	-709	-632	-494	177	0.65
Pb <sub>2</sub> V <sub>2</sub> O <sub>7</sub>	-521 -521 <sup>a)</sup>	-517	-462	-482	-606	-134	0.22

a) Reference data.<sup>8)</sup> All the values except  $\eta$  have a unit of ppm. The experimental errors of  $\delta_{\text{iso(MAS)}}$  in this work are  $\pm 0.5$  ppm. The experimental errors of  $\delta_{\text{iso(static)}}$ ,  $\delta_1$ ,  $\delta_2$ , and  $\delta_3$ , are  $\pm 10$  ppm for vanadates and  $\pm 20$  ppm for divanadates.

Sr<sub>3</sub>(VO<sub>4</sub>)<sub>2</sub> as the electronegativity of the divalent metal decreases in the order Pb > Zn > Mg > Ca > Sr > Ba. It is interesting to note that for vanadates containing two kinds of divalent metal atoms this relationship holds if the average electronegativity of two kinds of divalent metals is taken. It should be however pointed out here that in Sr<sub>3</sub>(VO<sub>4</sub>)<sub>2</sub> and Ba<sub>3</sub>(VO<sub>4</sub>)<sub>2</sub> the order is reversed, although the difference is very small. This reason is not clear at present because the precise structural parameters of Sr<sub>3</sub>(VO<sub>4</sub>)<sub>2</sub> are not known.

It is possible that the coordination number and the symmetry of the first coordination sphere of a divalent metal atom affect the <sup>51</sup>V shielding. The crystallographic data<sup>10–12)</sup> indicate that Mg<sub>3</sub>(VO<sub>4</sub>)<sub>2</sub> is isostructural with Zn<sub>3</sub>(VO<sub>4</sub>)<sub>2</sub> in which the coordination number of Zn<sup>2+</sup> is six. Sr<sub>3</sub>(VO<sub>4</sub>)<sub>2</sub> is isostructural with Ba<sub>3</sub>(PO<sub>4</sub>)<sub>2</sub><sup>22)</sup> in which the divalent metals take two different coordination numbers of ten and twelve. In Ba<sub>3</sub>(VO<sub>4</sub>)<sub>2</sub>, Ba<sup>2+</sup> ions also take two different coordination numbers of six and ten. In spite of this difference in the coordination number of the divalent cation, the plots come on the straight line as seen in Fig. 5, indicating that for the present divalent metal vanadates the electronegativity of the divalent metal is the most significant parameter dominating the <sup>51</sup>V shielding of VO<sub>4</sub>-tetrahedron.

**Crystalline Divanadates.** Figure 6 shows the plot of the isotropic chemical shift of divanadates determined by <sup>51</sup>V MAS NMR against Pauling's electronegativity of the divalent metal. In divanadates, the re-

lation between the  $\delta_{\text{iso}}$  and  $EN$  is not so simple as in vanadates. The structural unit of an divanadate group, V<sub>2</sub>O<sub>7</sub><sup>4-</sup>, is composed of two corner-sharing VO<sub>4</sub>-tetrahedra, and the vanadium sites are not always crystallographically equivalent. As can be seen in Fig. 4b, the <sup>51</sup>V MAS NMR spectra of Ca<sub>2</sub>V<sub>2</sub>O<sub>7</sub>, Zn<sub>2</sub>V<sub>2</sub>O<sub>7</sub>, and Pb<sub>2</sub>V<sub>2</sub>O<sub>7</sub> show only one isotropic chemical shift. In Zn<sub>2</sub>V<sub>2</sub>O<sub>7</sub> the number of the isotropic chemical shift is equal to the number of crystallographically equivalent vanadium site. In spite of the presence of two crystallographically inequivalent vanadium sites, Pb<sub>2</sub>V<sub>2</sub>O<sub>7</sub> also shows only one isotropic chemical shift, probably indicating that those vanadium sites are magnetically equivalent within the experimental resolution of the spectrum of 0.5 ppm.

The crystal structure of Mg<sub>2</sub>V<sub>2</sub>O<sub>7</sub> is schematically shown in Fig. 7. In this crystal, V<sub>2</sub>O<sub>7</sub><sup>4-</sup> anions are adjacent to each other, and a V<sub>2</sub>O<sub>7</sub><sup>4-</sup> consists of two crystallographically inequivalent vanadium sites; site 1 regarded as VO<sub>4</sub>-tetrahedron and site 2 regarded as VO<sub>5</sub>-trigonal bipyramid-like highly distorted VO<sub>4</sub>-tetrahedron. It is assumed that the presence of these sites gives rise to a large difference in two NMR chemical shifts at  $\delta = -551$  and  $-647$  as shown in Fig. 4b.

As seen from Fig. 1 and Table 1, the VO<sub>4</sub>-tetrahedron of site 2 is much more distorted than site 1 and the average V–O bond length of site 2 is larger than that of site 1. It is considered that the decrease in the average V–O bond length and results in the increase in the shielding of a vanadium nucleus against the exter-

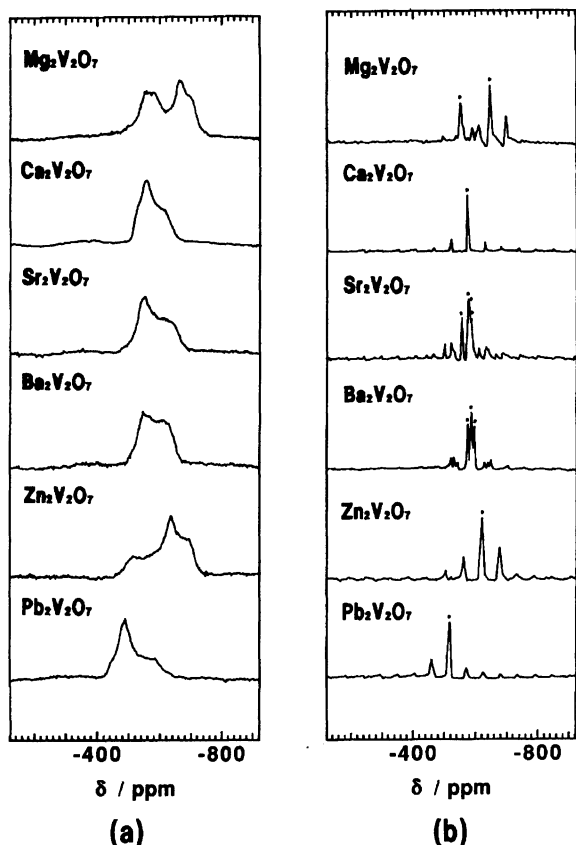


Fig. 4.  $^{51}\text{V}$  static (a) and MAS (b) NMR spectra of various crystalline divanadates. Isotropic chemical shifts are indicated by asterisks.

nal magnetic field causing the lower frequency shift of  $^{51}\text{V}$ . Accordingly, it may be reasonable to assign the peak at  $\delta = -551$  to site 2 and the peak at  $\delta = -647$  to site 1. This interpretation is also based upon the finding that the  $^{51}\text{V}$  shielding in the  $\text{VO}_4$ -tetrahedron increases with decreasing average V–O bond length and increasing degree of structural symmetry.<sup>23)</sup>

The  $^{51}\text{V}$  MAS NMR spectrum of  $\text{Sr}_2\text{V}_2\text{O}_7$  has four isotropic chemical shifts at  $\delta = -561$ ,  $-581$ ,  $-584$ , and  $-593$  as seen in Fig. 4b. These should correspond to the four crystallographically inequivalent vanadium sites in  $\text{Sr}_2\text{V}_2\text{O}_7$ . An exact assignment of each isotropic chemical shifts to corresponding site cannot be made at present, because the crystallographic difference between the sites is not so obvious. This is also the case for  $\text{Ba}_2\text{V}_2\text{O}_7$ .

It is known that  $\text{V}_2\text{O}_7^{4-}$  groups in crystalline  $\text{M}_2\text{V}_2\text{O}_7$  can be classified into two types, thortveitite-type with a staggered configuration and dichromate-type with an eclipsed configuration, as shown in Fig. 8.<sup>17)</sup> Baglio and Dann<sup>16)</sup> found that the difference in configuration is closely related to the ionic radius of the divalent cation. In thortveitite-type  $\text{Mg}_2\text{V}_2\text{O}_7$  and  $\text{Zn}_2\text{V}_2\text{O}_7$  crystals the cationic radius is smaller than that of calcium ion, while in dichromate-type  $\text{Sr}_2\text{V}_2\text{O}_7$ ,  $\text{Ba}_2\text{V}_2\text{O}_7$ , and  $\text{Pb}_2\text{V}_2\text{O}_7$  crystals it is

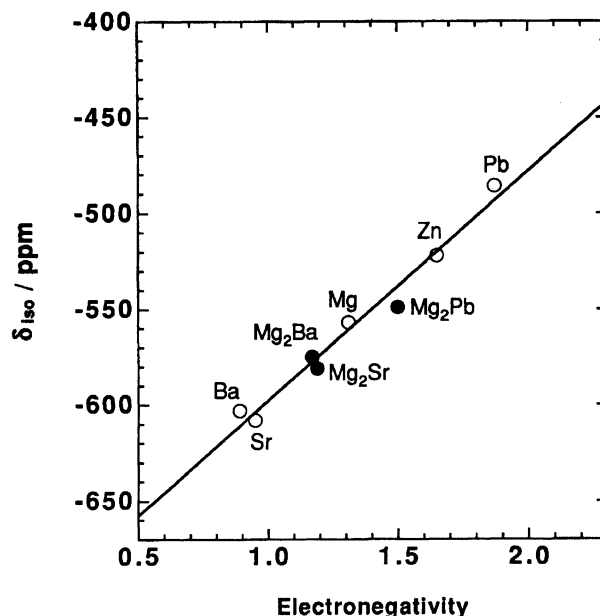


Fig. 5. Plots of the isotropic chemical shift determined from  $^{51}\text{V}$  MAS NMR spectra vs. Pauling's electronegativity of divalent metal (M) for vanadates ( $\text{M}_3(\text{VO}_4)_2$ ):  $\circ$  and ( $\text{Mg}_2\text{M}(\text{VO}_4)_2$ ):  $\bullet$ .

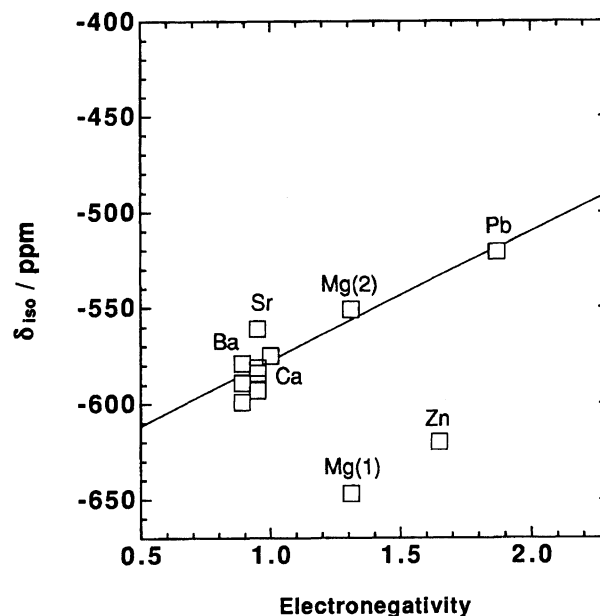


Fig. 6. Plots of the isotropic chemical shift determined from  $^{51}\text{V}$  MAS NMR spectra vs. Pauling's electronegativity of divalent metal (M) for divanadates ( $\text{M}_2\text{V}_2\text{O}_2$ ):  $\square$ . The line indicates the relation between  $\delta_{\text{iso}}$  and  $EN$  for the divanadates of dichromate-type configuration.

larger.<sup>13–18)</sup> As seen from Table 2, the sign of the chemical shift anisotropy,  $\Delta\delta$ , is positive in  $\text{Zn}_2\text{V}_2\text{O}_7$  while that is negative in  $\text{Sr}_2\text{V}_2\text{O}_7$  and  $\text{Pb}_2\text{V}_2\text{O}_7$ . This implies that the sign of  $\Delta\delta$  is related to the configuration; i.e.,  $\Delta\delta > 0$  in thortveitite-type and  $\Delta\delta < 0$  in dichromate-

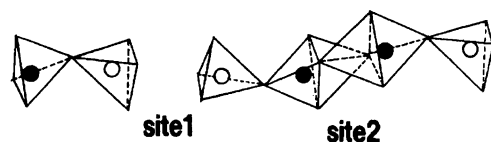


Fig. 7. The arrangement of anions in the structure of  $\text{Mg}_2\text{V}_2\text{O}_7$ . The open circles and the closed circles represent site 1 and site 2, respectively.

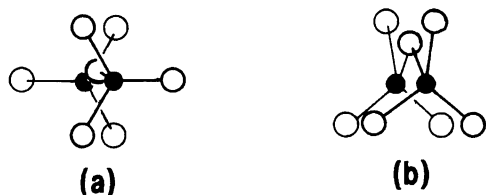


Fig. 8. Two types of crystalline divanadates.<sup>17)</sup> (a) thortveitite and (b) dichromate. The large open circles and small closed circles represent oxygen atoms and vanadium atoms, respectively.

type. The negative sign of the chemical shift anisotropy for  $\text{Ca}_2\text{V}_2\text{O}_7$ , whose crystal structure is not known, indicates that the structural unit ( $\text{V}_2\text{O}_7^{4-}$ ) may be of the dichromate-type, as suggested by Baglio and Dann.<sup>16)</sup>

A difference in  $^{51}\text{V}$  chemical shift between the thortveitite-type and dichromate-type divanadates will be discussed. The  $^{51}\text{V}$  chemical shifts for the former type are lower frequencies than those for the latter to a considerable extent. It is known that for various crystalline silicates the  $^{29}\text{Si}$  isotropic chemical shifts are closely correlated with the Si-O-Si bond angle via the s-character of oxygen.<sup>24)</sup> As seen from Table 2, a similar reasoning may be valid for divanadates, that is, the V-O-V angle may be a major structural parameter causing the difference in the  $^{51}\text{V}$  shielding between the two types of divanadates. The degree of s-hybridization, %s, of the oxygen bond orbitals in the M-O-M bonds in given by the well known equation,

$$\%s = 100 \times \cos \theta / (\cos \theta - 1) \quad (15)$$

where  $\theta$  is the V-O-V bond angle. The %s is typically 34.6–36.8 % for  $\theta = 122^\circ$ – $125.6^\circ$  which correspond to dichromate-type, while it increases up to 46.2 % for  $\theta = 149.3^\circ$  which correspond to the thortveitite-type  $\text{Zn}_2\text{V}_2\text{O}_7$ . Since the s orbital has a higher shielding against the external magnetic field, an increase in the V-O-V bond angle and the resulting increase in s-hybridization may be the main reason for the lower frequency shift of  $^{51}\text{V}$  in thortveitite-type divanadates in a similar manner as  $^{29}\text{Si}$  NMR.<sup>24)</sup> This implies that for divanadates containing various divalent metal cations the  $^{51}\text{V}$  chemical shift is affected not only by the electronegativity of the divalent metal cation but also by the V-O-V angle.

By assuming a linear relationship between the  $\delta_{\text{iso}}$  and  $EN$  for divanadates of dichromate-type configura-

tion as shown in Fig. 6, this relationship is expressed by the following equation,

$$\delta_{\text{iso}} = 67.2 \times (EN - 9.61) \quad (16)$$

For  $\text{Sr}_2\text{V}_2\text{O}_7$  and  $\text{Ba}_2\text{V}_2\text{O}_7$  having a number of  $\delta_{\text{iso}}$ , the average  $\delta_{\text{iso}}$  was used. The slope of 67.2 for divanadates is about one half that of 122 for vanadates shown in Fig. 5. It is reasonable to assume that the slope of the straight line is correlated with the degree of the effect of electronegativity of the divalent metal on the  $^{51}\text{V}$  isotropic chemical shift,  $\delta_{\text{iso}}$ . In divanadates two  $\text{VO}_4$ -tetrahedra are linked together by sharing their corner. Accordingly, the influence of the second neighboring divalent cations on the  $^{51}\text{V}$  shielding may be less.

### Summary

$^{51}\text{V}$  static and MAS NMR spectra of crystalline divalent metal vanadates  $\text{M}_3(\text{VO}_4)_2$  ( $\text{M} = \text{Mg}, \text{Sr}, \text{Ba}, \text{Zn}, \text{Pb}$ ) and  $\text{Mg}_2\text{M}'(\text{VO}_4)_2$  ( $\text{M}' = \text{Sr}, \text{Ba}, \text{Pb}$ ) and divanadates  $\text{M}_2\text{V}_2\text{O}_7$  ( $\text{M} = \text{Mg}, \text{Ca}, \text{Sr}, \text{Ba}, \text{Zn}, \text{Pb}$ ) were measured. The following conclusions were drawn.

(1) The  $^{51}\text{V}$  isotropic chemical shifts depend on various parameters such as components present in each vanadate, oxygen coordination state around a vanadium atom and configuration and polymerization degree of a vanadate anion.

(2) The  $^{51}\text{V}$  isotropic chemical shifts decrease almost linearly with decreasing electronegativity of the divalent metal adjacent to the  $\text{VO}_4$ -tetrahedron. This indicates that in vanadates the electronegativity of the divalent metal atom dominates the  $^{51}\text{V}$  isotropic chemical shifts.

(3) The similar trend was also observed in divanadates of dichromate-type, although the slope of the linear relation is less in divanadates than in vanadates.

(4) In divanadates the isotropic chemical shifts appear at lower frequencies in the thortveitite-type configuration than in the dichromate-type configuration. This is explained by assuming that the degree of s-hybridization of the oxygen orbitals in the V-O-V bonds is higher in the thortveitite-type than in the dichromate-type.

The authors thank Professor Fumitaka Horii and Mrs Kyoko Omine of Kyoto University for their helpful advice and assistance in the NMR measurements. This work was supported by a Grant-in-Aid for Scientific Research No. 02403016 from the Ministry of Education, Science and Culture.

### References

- 1) H. Hirashima, Y. Watanabe, and T. Yoshida, *J. Non-Cryst. Solids*, **95&96**, 825 (1987).
- 2) A. Talledo, A. M. Anderson, and C. G. Granqvist, *J. Appl. Phys.*, **69**, 3261 (1991).
- 3) R. J. Colton, A. M. Guzman, and J. W. Rabalais, *J. Appl. Phys.*, **49**, 409 (1978).

- 4) D. Mouhssine, D. Michel, and T. Daniel, *Rev. Chim. Miner.*, **23**, 746 (1986).
  - 5) R. C. Powell, S. A. Payne, L. L. Chase, and G. D. Wilke, *Phys. Rev. B*, **B41**, 8593 (1990).
  - 6) E. Oldfield, R. A. Kinsey, B. Montez, T. Ray, and K. A. Smith, *J. Chem. Soc., Chem. Commun.*, **1982**, 254.
  - 7) V. M. Mastikhin and O. B. Lapina, *React. Kiner. Catal. Lett.*, **24**, 119 (1984).
  - 8) H. Eckert and I. E. Wachs, *J. Phys. Chem.*, **93**, 6796 (1989).
  - 9) S. Hayashi and K. Hayamizu, *Bull. Chem. Soc. Jpn.*, **63**, 961 (1990).
  - 10) R. Gopal and C. Calvo, *Can. J. Chem.*, **49**, 3056 (1971).
  - 11) N. Krishnamachari and C. Calvo, *Can. J. Chem.*, **49**, 1629 (1971).
  - 12) R. Susse and M. J. Buerger, *Z. Kristallogr.*, **131**, 161 (1970).
  - 13) R. D. Shannon and C. Calvo, *Can. J. Chem.*, **51**, 70 (1973).
  - 14) R. Gopal and C. Calvo, *Can. J. Chem.*, **51**, 1004 (1973).
  - 15) R. Gopal and C. Calvo, *Acta Crystallogr., Sect. B*, **B30**, 2491 (1974).
  - 16) J. A. Baglio and J. N. Dann, *J. Solid State Chem.*, **4**, 87 (1972).
  - 17) I. D. Brown and C. Calvo, *J. Solid State Chem.*, **1**, 173 (1970).
  - 18) F. C. Hawthorne and C. Calvo, *J. Solid State Chem.*, **26**, 345 (1978).
  - 19) K. A. Smith, R. J. Kirkpatrick, E. Oldfield, and D. M. Henderson, *Am. Mineral.*, **68**, 1206 (1983).
  - 20) C. P. Slichter, "Principles of Magnetic Resonance," 3rd ed, Springer-Verlag, Tokyo (1989), pp. 605—616.
  - 21) N. Bloembergen and T. J. Rowland, *Acta Metall.*, **1**, 731 (1953).
  - 22) W. H. Zachariasen, *Acta Crystallogr.*, **1**, 263 (1948).
  - 23) S. Hayakawa, T. Yoko, and S. Sakka, submitted to *J. Solid State Chem.*
  - 24) G. Engelhardt and R. Radeaglia, *Chem. Phys. Lett.*, **108**, 271 (1984).
-